Some Analysis in Distributed MIMO Systems

Huaiyu Dai

Department of Electrical and Computer Engineering, NC State University, Raleigh, NC 27695 USA
Email: Huaiyu_Dai@ncsu.edu

Hongyuan Zhang and Quan Zhou

Marvell Semiconductor Inc., 5488 Marvell Lane, MS 2-401, Santa Clara, CA 95054 USA
Email: {hongyuan, quanzhou}@marvell.com

Abstract—**The predicted capacity gain of a traditional co-located MIMO system is often severely limited in realistic propagation scenarios, especially when the number of antennas becomes large. Recently, a generalized paradigm for multiple-antenna communications, distributed MIMO, is proposed as a remedy. In this paper, through asymptotic large-system analysis, we provide solid justifications on the advantages of distributed MIMO over co-located MIMO when communication channels are subject to spatial correlation and shadow fading. We also exploit inherent macrodiversity in distributed MIMO to devise a cost-effective link adaptation scheme that achieves significant performance gain.**

Index Terms—**capacity, distributed antenna, MIMO systems, shadowing, spatial correlation**

I. INTRODUCTION

Recently, the remarkable capacity potential of wireless systems with antenna arrays at both the transmitters and receivers, called multiple-input multiple-output (MIMO) systems, was unveiled [1][2]. The capacity gain of MIMO systems is realized through spatial multiplexing; in the ideal scenario, an N by N MIMO system can increase spectral efficiency by a factor of N relative to single-antenna systems. Substantial effort has been devoted to incorporating MIMO technology into emerging communication standards, including the high-speed downlink packet access (HSDPA) mode of third-generation cellular networks (UMTS), IEEE 802.11n for next-generation wireless local-area networks (WLAN), and IEEE 802.16 for outdoor fixed/nomadic wireless wide-area networks (WWAN) [3].

MIMO techniques are anticipated to be widely employed in future wireless networks to address the ever-increasing capacity and quality demands. The main question is whether the enormous gains predicted can be achieved in realistic environments. In other words, if we keep adding antennas into MIMO systems, can we keep obtaining expected returns even if the increased cost in deployment, hardware and computation can be afforded?

Unfortunately the answer is no, if the antennas are to be packed together with spacing on the order of wavelength in the traditional way.

The leading reason comes from spatial correlation due to existence of few dominant scatterers, small angle spread, and insufficient antenna spacing [1]. Usually situations are more stringent at the base station side for outdoor deployment, where antennas are elevated and unobstructed by local scatterers, and antenna spacing has to be reduced due to environmental concerns when more antennas are added. Generally, spatial correlation increases the condition number (i.e., spreads out the singular value distribution) of the channel matrix. The loss thus incurred can be measured in two ways. The concept of effective degrees of freedom proposed in [4] discards eigenmodes with negligible capacity at a given signal-to-noise ratio (SNR), while in [5] the loss in growth rate (spectral efficiency per antenna) is evaluated as the number of antennas goes to infinity. In the extreme case (e.g. the keyhole effect [1]), the channel rank is hard-limited by the few independent propagation paths, so putting more antennas can by no means increase spatial degrees of freedom, though other advantages like diversity and array gains may still be preserved.

Another reason may be less obvious. Current study of MIMO systems seldom explicitly addresses the shadow fading issues, though it is natural to expect severely diminished link quality when unfavorable shadowing is experienced. Multiple antennas sited in the same locale experience the same shadowing thus cannot improve the situation.

A generalized paradigm for multiple-antenna communications, distributed MIMO (D-MIMO), has been proposed to address the problems inherent in the traditional co-located MIMO (C-MIMO) systems [6][7]. As depicted in Fig. 1, the key difference between D-MIMO and C-MIMO is that multiple antennas for one end of communications are *distributed* among multiple *widely-separated* radio ports, and *independent* large-scale fading is experienced for each link between a mobile-port pair. As understood in Fig. 1 from a downlink viewpoint, a D-MIMO system can be represented with a triplet of (K, M, N), while a C-MIMO can be viewed as a $(1, KM, N)$ D-MIMO. The multiple ports may have the

same functionality as base stations in today's cellular system, or may be realized as remote antennas, i.e., small devices containing antennas and electric-optic converters which relay the radio signal to a control unit in the access network. Our illustration will focus on this *downlink* cellular scenario, but our results will apply largely to other situations as well, such as distributed MIMO equivalently formed through cooperation among mobile users or wireless sensor nodes. Unless noted, we will mainly consider a $(M, 1, N)$ D-MIMO for simplicity, and compare it with a $(1, M, N)$ C-MIMO.
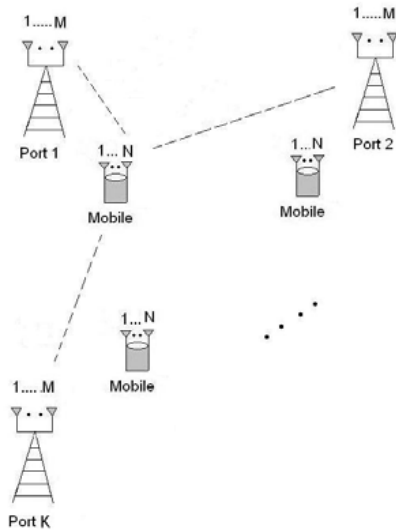

Fig. 1 Distributed MIMO Systems

The generalization from C-MIMO to D-MIMO offers many advantages. In this paper, the aforementioned spatial correlation and shadow fading issues will be particularly addressed. D-MIMO can also be regarded as a generalization of distributed antenna system (DAS), whose study dates back to [8], and has attracted attention recently due to its power and capacity advantage over the centralized configuration in broadband wireless network [9]. Most work on DAS so far has emphasized on its advantages in practical employment, such as lower transmit power, uniform and enhanced coverage, and ease of cell planning.

This paper is organized as follows. In Section II, some preliminaries on MIMO systems, including their capacity and modeling, are given. Our analysis on the impact of spatial correlation and shadow fading is presented in Section III and IV, respectively. In Section IV, it is also shown how macrodiversity inherent in D-MIMO can be effectively explored to adapt the data transmission for better system performance with reasonable cost. Finally, Section V concludes the paper with some future research directions.

II. MIMO SYSTEM

A. MIMO Capacity

Consider a general MIMO system given by

$$\mathbf{y} = \mathbf{H}\mathbf{x} + \mathbf{n} , \qquad (1)$$

where $\mathbf{y}$ is the received vector corresponding to the outputs of N receive antennas, $\mathbf{x}$ contains the substreams transmitted by M transmit antennas, $\mathbf{H}$ is an $N \times M$ random matrix that captures the channel characteristics between transmit and receive antenna arrays, whose modeling is detailed in II.B, and $\mathbf{n}$ is an N-dimensional noise vector of independent and identically distributed (i.i.d.) zero-mean complex Gaussian random variables with unit variance. The total transmit power is constrained as $\mathrm{tr}(E[\mathbf{x}\mathbf{x}^H]) = \mathrm{tr}(\mathbf{\Sigma}) \leq \rho$. For sake of illustration, we will focus on the flat-fading channel with white Gaussian noise in this paper. But the results are readily extended to the wideband frequency-selective fading and/or non-white noise scenarios.

The mutual information of the instantaneous MIMO channel (1) is given by

$$I(\mathbf{H}) = \log \det \left(\mathbf{I} + \mathbf{H}\mathbf{\Sigma}\mathbf{H}^H \right) \qquad (2)$$

with a Gaussian codebook. If channel $\mathbf{H}$ is known at the transmitter, water-filling power allocation achieves the instantaneous channel capacity, denoted as $C(\mathbf{H})$. Otherwise, equal power allocation $\mathbf{\Sigma} = (\rho/M)\mathbf{I}_M$ is often assumed, yielding $I_{eq}(\mathbf{H})$.

For fading channels there are two distinct notions of capacity: ergodic capacity and outage capacity [2]. Ergodic capacity is the maximum mutual information averaged over all channel states. When the channel is perfectly known both at the transmitter and the receiver, the ergodic capacity is given by $C_{WF} = E_{\mathbf{H}}[C(\mathbf{H})]$. When the channel is known at the receiver but not at the transmitter, it is known

$$(\rho/M)\mathbf{I}_M = \arg\max_{\mathbf{\Sigma}:tr(\mathbf{\Sigma})\leq\rho} E_{\mathbf{H}}[I(\mathbf{H})] ,$$

and the ergodic capacity is given by $C_{eq} = E_{\mathbf{H}}[I_{eq}(\mathbf{H})]$. We will mainly assume equal power allocation among transmitted substreams in our study.

For delay-constrained applications where the data rate cannot be adapted with channel variations, it is often meaningful to study the outage capacity $C^{(p)}$, defined with respect to an outage probability p implicitly through $p = P\left(I(\mathbf{H}) < C^{(p)}\right)$.

B. Channel Modeling

MIMO capacity depends crucially on the realization of the channel matrix. In indoor environments with rich scattering, the channel matrix can be safely modeled as $\mathbf{H}_w$, each column of which is i.i.d. with distribution $\mathcal{CN}(\mathbf{0}, \mathbf{I}_M)$[1].

A common approach to account for spatial correlation in the physical channel is to model the channel matrix as

$$\mathbf{H} = \mathbf{A}_R \mathbf{A}_T^H , \qquad (3)$$

---

[1] $\mathcal{CN}(\mathbf{0}, \mathbf{\Sigma})$ denotes a circularly symmetric complex Gaussian distribution with zero mean and covariance matrix $\mathbf{\Sigma}$. $\mathcal{N}(\cdot, \cdot)$ denotes a real Gaussian distribution.

where $\mathbf{A}_T = [\mathbf{a}_{T1}, \mathbf{a}_{T2}, ... \mathbf{a}_{TL}]$ is an $M \times L$ matrix representing scattering characteristics at the transmit end, while $\mathbf{A}_R = [\mathbf{a}_{R1}, \mathbf{a}_{R2}, ... \mathbf{a}_{RL}]$ is a corresponding $N \times L$ matrix at the receive end, and L denotes the number of significant paths between them. Depending on the local scattering conditions, the columns of $\mathbf{A}_T$ and $\mathbf{A}_R$ can be modeled as fixed array-response vectors (no scattering), white Gaussian vectors (rich scattering), or correlated Gaussian vectors (fading correlation). This generalized channel model includes many interesting scenarios in practice, such as the separable correlation model and the keyhole effect.

In this paper, without loss of generality, we will focus on spatial correlation at the base stations or radio ports, i.e., the transmit side, so $\mathbf{A}_R = \mathbf{H}_w$. This readily addresses outdoor cellular macrocell environments, where mobile terminals are surrounded by rich scatterers while antenna arrays at the base stations are elevated above urban clusters and far away from local scattering. Extensions to other scenarios are straightforward. In particular, we will consider the following two models.

(1) An extreme scenario where $L = 1$ and $\mathbf{A}_T$ is the single dominant fixed transmit steering vector.

(2) $L = M$ and $\mathbf{H} = \mathbf{H}_w \mathbf{R}_T^{1/2}$ with some deterministic Hermitian matrix $\mathbf{R}_T$. That is, each column of $\mathbf{A}_T$ is i.i.d. with distribution $\mathcal{CN}(\mathbf{0}, \mathbf{R}_T)$, and $\mathbf{R}_T$ is thus called transmit correlation matrix. In this paper, uniform linear arrays are assumed, dictating a Toeplitz structure for $\mathbf{R}_T$:

$$\{\mathbf{R}_T\}_{ij} \triangleq \rho_{j-i} = \rho_{i-j}^*. \tag{4}$$

To address the large-scale fading effect, we introduce a diagonal matrix $\mathbf{\Phi}$. Without loss of generality, we exclude the path loss effect and assume i.i.d. shadow fading for different ports of D-MIMO. Thus for C-MIMO $\mathbf{\Phi} = \Phi \mathbf{I}_M$; while for D-MIMO $\mathbf{\Phi} = \text{diag}(\Phi_1, \cdots, \Phi_M)$. The shadow fading coefficient is usually modeled as $\Phi = e^Y$ where $Y \sim \mathcal{N}(\lambda\mu_L, (\lambda\sigma_L)^2)$, with μ_L (dB) the area mean, σ_L (dB) the decibel spread, and $\lambda = \ln 10/10$. The cumulative distribution function of Φ is given by

$$F_\Phi(x) = 1 - Q\left(\frac{\ln x - \lambda\mu_L}{\lambda\sigma_L}\right), \tag{5}$$

where $Q(\cdot)$ is the standard Gaussian tail function. We also have

$$E\{\Phi\} = e^{\lambda\mu_L + \frac{\lambda^2\sigma_L^2}{2}} \text{ and } E\{\Phi^2\} = e^{2\lambda\mu_L + 2\lambda^2\sigma_L^2}. \tag{6}$$

To avoid confounding effects, in Section III we will focus on spatial correlation by assuming model (3), while in Section IV we will study the impact of shadow fading by assuming

$$\mathbf{H} = \mathbf{H}_w \mathbf{\Phi}^{1/2}. \tag{7}$$

A joint study on both effects constitutes our future work.

Our study focuses on the asymptotic scenario that the total number of transmit or receive antennas goes to

infinity. Besides analytical tractability through laws of large numbers, central limit theorem, and random matrix theory, the study of large system performance also has practical advantages: what is revealed in the asymptotic limit is fundamental in nature, which may be concealed in the finite case by random fluctuations and other transient properties of the matrix entries; moreover, the convergence to the asymptotic limit is typically rather fast as the system size grows. We also focus our study on the high SNR regimes.

In the following, when convergence of a sequence of random variables is involved, shorthand notation "D" stands for in distribution, and "a.s." for almost surely. "log" is used for logarithm with an arbitrary base, and "ln" for base e.

III. IMPACT OF SPATIAL CORRELATION

First, let us consider the extreme model (1) in II.B for the channel between each radio port and a mobile. Essentially a C-MIMO system sees a rank-1 channel and assumes no advantage in spatial multiplexing gain over a single-input single output (SISO) system. In contrast, based on the geometry of D-MIMO, each radio port provides at least one independent link even in the absence of remote scattering objects. If $K > M$, the single-user D-MIMO channel is guaranteed to have full rank. This is verified in Fig. 2 with a 4×4 configuration. We can see that C-MIMO achieves only 1 more bits/s/Hz in ergodic capacity for every 3 dB gain in SNR. On the other hand, the channel rank and thus the communication dimensions quickly build up with antennas distributed among separated radio ports in D-MIMO, achieving 2 and 4 more bits/s/Hz for every 3 dB gain in SNR for $(2,2,4)$ and $(4,1,4)$ D-MIMO, respectively. It is found in [11] that unlike the SISO case, delay spread channels offer advantages over flat-fading channels in terms of ergodic capacity for C-MIMO systems. This conclusion is a result of the assumption that delay paths tend to increase the total angle spread, and thus improve the channel rank. In D-MIMO, however, the full rank can be obtained even with the flat-fading channel, due to its inherent large angle spread and wide antenna spacing.
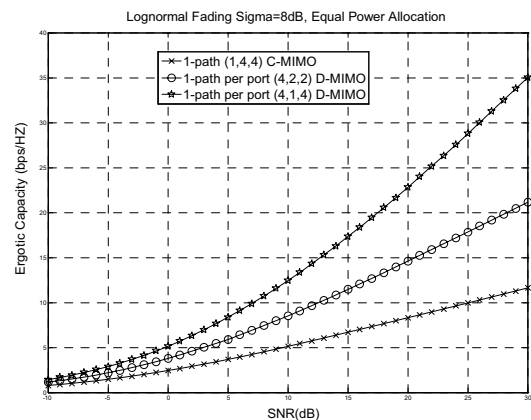

Fig. 2 Ergodic capacity of 4×4 MIMO systems in rank-deficient propagation environments

We now turn to model (2) in II.B for more in-depth analysis. We follow the approach in [5] to study the asymptotic capacity loss per spatial dimension due to fading correlation. For ease of exposition we consider a square channel matrix ($M = N$) with equal power allocation, and examine

$$I^0 = \lim_{M \to \infty} \frac{I_{eq}(\mathbf{H})}{M} = \lim_{M \to \infty} \frac{1}{M} \log \det \left(\mathbf{I} + \frac{\rho}{M} \mathbf{H}_w \mathbf{R}_T \mathbf{H}_w^H \right). \quad (8)$$

As is known from random matrix theory, (8) is insensitive to channel realizations for large M. At high SNR, the loss in I^0 can be nicely quantified as

$$\Delta I^0 = \int_0^1 \log S_T(f) df, \quad (9)$$

where $S_T(f) = \sum_i \rho_i e^{j2\pi if}$ is the spectral density of the Toeplitz matrix $\mathbf{R}_T$. The underlying rationale is that the distribution of the eigenvalues of $\mathbf{R}_T$ asymptotically (as $M \to \infty$) approaches $S_T(f)$ on $[0,1]$ [10].

First let us consider a somewhat simplified model for $\mathbf{R}_T$ for some complex number η with $|\eta| \leq 1$:

$$\rho_i = \eta^i. \quad (10)$$

In this case

$$S_T(f) = \frac{1 - |\eta|^2}{|1 - \eta e^{i2\pi f}|^2}. \quad (11)$$

A complex integral calculation reveals

$$\Delta I^0 = \log \left(1 - |\eta|^2\right). \quad (12)$$

This simple model tells quite a bit about capacity loss due to spatial correlation: it is a monotonic decreasing function of the correlation coefficient η between two adjacent antenna elements, and the loss goes without bound as in (12).

Next let us examine a more practical model [11]

$$\rho_i = e^{-j2\pi i\Delta \cos(\bar{\theta})} \cdot q^{i^2}, \text{ with } q = e^{-(1/2)(2\pi\Delta\sin(\bar{\theta})\sigma_\theta)^2}, \quad (13)$$

where Δ is the relative antenna spacing with respect to the wavelength, $\bar{\theta}$ is the mean angle of departure, and σ_θ is a parameter reflecting the angle spread, all for the transmit array. In this case we have

$$S_T(f) = \vartheta_3(\pi(f - \Delta \cos \bar{\theta}), q) \quad (14)$$

where $\vartheta_3(\cdot, \cdot)$ is the third-order theta function given in [12]. Using the following expansion

$$\vartheta_3(u, q) = \prod_{n=1}^{\infty} (1 - q^{2n})((1 + 2q^{2n-1} \cos 2u + q^{2(2n-1)}), \quad (15)$$

we get

$$\Delta I^0 = \sum_{n=1}^{\infty} \log(1 - q^{2n}) = \frac{1}{3} \log\left(\frac{1}{2} \vartheta_1'(0, q)\right) - \frac{1}{12} \log q, \quad (16)$$

where $\vartheta_1'(\cdot, \cdot)$ is the derivative of the first-order theta function. A schematic demonstration of (16) is given in Fig. 3.
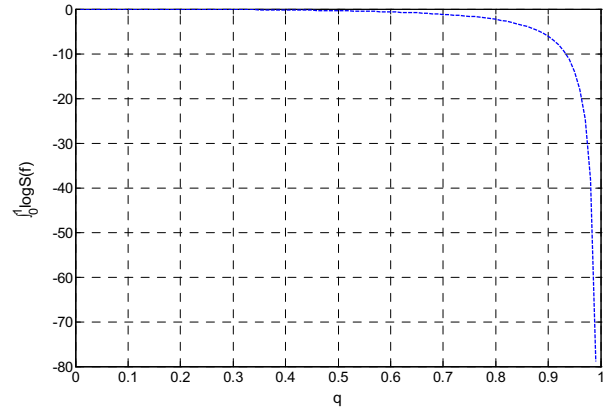

Fig. 3 Capacity Loss due to Fading Correlation

Again, it is a monotonic decreasing function of q, but by the definition of q and the above quantitative results, we will be able to directly relate the capacity loss with the environmental and system parameters including the angle spread and antenna spacing. Specifically, we observe that D-MIMO simultaneously enlarges the antenna spacing Δ and angle spread σ_θ, rendering a q small enough to incur negligible loss. We can also calculate the critical antenna spacing, or the optimal antenna number for a given aperture and propagation environment, just to name a few applications.

IV. IMPACT OF SHADOW FADING

Properly normalized, shadow fading should not have impact on the ergodic capacity for C-MIMO, but its induced variance should deteriorate the outage capacity. Our results of the impact of shadow fading on outage capacity are presented in IV.A. In the analysis, we will use the fact that, if $I(\mathbf{H}) \sim \mathcal{N}(\mu, \sigma^2)$, the outage probability

$$p = Q((\mu - C^{(p)})/\sigma). \quad (17)$$

A. Outage Capacity

We differentiate two scenarios, (1) large M and fixed N, (2) large M and N with their ratio fixed, and summarize our results as two theorems below, whose proofs are deferred to the appendix.

Theorem 1: For large M, ρ and fixed N, as $M \to \infty$, the outage capacity

(1) for C-MIMO with pure Rayleigh fading is given by

$$C_{C,R}^{(p)} = \mu_1 - \sigma_1 Q^{-1}(p); \quad (18)$$

(2) for C-MIMO with Rayleigh fading and Log-normal shadowing is given by

$$C_{C,S}^{(p)} = (\mu_1 + N\lambda\mu_L \log e) - \sqrt{\sigma_1^2 + N^2\lambda^2\sigma_L^2 \log^2 e} Q^{-1}(p); \quad (19)$$

(3) for D-MIMO with Rayleigh fading and Log-normal shadowing is given by

$$C_{D,S}^{(p)} = \left[\mu_1 + N \left(\lambda \mu_L + \frac{\lambda^2 \sigma_L^2}{2} \right) \log e \right]$$
$$- \log e \sqrt{\frac{N}{M} [(1+N) e^{\lambda^2 \sigma_L^2} - N] Q^{-1}(p)}. \qquad (20)$$

In the above

$$\mu_1 = N \log(1 + \rho) \approx N \log \rho \qquad (21)$$

and

$$\sigma_1 = \sqrt{\frac{N}{M}} \frac{\rho \log e}{(1+\rho)} \approx \sqrt{\frac{N}{M}} \log e . \qquad (22)$$

Proof: See Appendix A.

Remark: In all cases, the first term denotes the mean (ergodic) capacity due to symmetry of involved distributions, whose difference is somewhat related to the artifacts in the definition of shadowing parameters. What is of more interest is the difference in the second term. We observe that there is a non-vanishing component in the coefficient of $Q^{-1}(p)$ in (19) when $M \to \infty$, verifying the detrimental effect of shadowing fading on the C-MIMO outage capacity. The corresponding part fades away in D-MIMO thanks to its inherent macrodiversity.

Theorem 2: For large M, N, ρ, as $M, N \to \infty$, with $M/N \to \beta$, the outage capacity

(1) for C-MIMO with pure Rayleigh fading is given by

$$C_{C,R}^{(p)} = \mu_2 - \sigma_2 Q^{-1}(p) ; \qquad (23)$$

(2) for C-MIMO with Rayleigh fading and Log-normal shadowing is given by

$$C_{C,S}^{(p)} = (\mu_2 + \min(M,N) \lambda \mu_L \log e)$$
$$- \sqrt{\sigma_2^2 + \min^2(M,N) \lambda^2 \sigma_L^2 \log^2 e} Q^{-1}(p); \qquad (24)$$

(3) for D-MIMO with Rayleigh fading and Log-normal shadowing is given by

$$C_{D,S}^{(p)} = \begin{cases} C_{D,S}^{(p)} = (\mu_2 + M \lambda \mu_L \log e) \\ \quad - \sqrt{\sigma_2^2 + M \lambda^2 \sigma_L^2 \log^2 e} Q^{-1}(p) & \beta \le 1 \\ \mu_D - \sigma_D Q^{-1}(p) & \beta > 1 \end{cases} \qquad (25)$$

where

$$\mu_D = N \left[\log \frac{\rho}{e} + \beta E_\Phi \{ \log(1 + C_2 \Phi) \} - \log C_2 \beta \right], \qquad (26)$$

with C_2 the solution to $E \{ C_2 \Phi / (1 + C_2 \Phi) \} = 1/\beta$, and σ_D is the standard deviation of $\sum_{i=1}^{N} \log \lambda_i$, with $\{\lambda_i\}$ the nonzero eigenvalues of $\mathbf{H}_w \mathbf{\Phi} \mathbf{H}_w^H$.

In the above

$$\mu_2 = \begin{cases} M \left[\log \frac{\rho}{e} + \log \frac{1-\beta}{\beta} + \frac{1}{\beta} \log \frac{1}{1-\beta} \right] & \beta < 1 \\ N \log \frac{\rho}{e} & \beta = 1 \\ N \left[\log \frac{\rho}{e} + (\beta-1) \log \frac{\beta}{\beta-1} \right] & \beta > 1 \end{cases} \qquad (27)$$

and (γ is the Euler constant)

$$\sigma_2 = \begin{cases} \log e \sqrt{\ln \frac{1}{1-\beta}} & \beta < 1 \\ \log e \sqrt{\ln N + \gamma + 1} & \beta = 1 \\ \log e \sqrt{\ln \frac{\beta}{\beta-1}} & \beta > 1. \end{cases} \qquad (28)$$

Proof: See Appendix B.

Remark: Though more involved, these results are qualitatively similar to those in Theorem 1. An improvement in outage capacity is observed again for D-MIMO with shadow fading for $\beta \le 1$. Closed-forms results for $\beta > 1$ are not available currently, but similar improvement is expected.

B. Link Adaptation

In last subsection, advantage of D-MIMO over C-MIMO in terms of outage capacity subject to shadow fading is demonstrated, due to inherent macrodiversity in D-MIMO. In this section, we explore a relevant topic, link adaptation for D-MIMO. Our scheme only utilizes the knowledge of large-scale fading, which is locally stationary and varies much more slowly than the detailed small-scale fading requested by the optimal approach based on singular value decomposition (SVD) of the channel. Therefore, estimation, feedback and update of channel state information (CSI) can be done on the order of the coherence time of the large-scale fading, with a fairly reasonable system overhead.

For simplicity, we only consider uncoded modulation, and the adaptive transmission parameters are the data rates and power levels of links between a mobile and its surrounding ports. Implicitly, the number of simultaneously transmitted data streams (and thus actively utilized antennas and radio ports) is also adapted according to the channel conditions.

Given large-scale fading coefficients $\{\Phi_k\}$ of the M links in D-MIMO, our bit and power allocation with $\sum_{k=1}^{M} b_k = B$ and $\sum_{k=1}^{M} P_k = P$ mainly comprises the following two steps:

1. Total transmit bits are allocated over subchannels so that the total transmit power is minimized for the same target bit error rate (BER). The basic idea is to put each unit of bits to the subchannel with least required energy. Initially bits will be assigned to the best subchannel (with largest channel gain), but later on there is a tradeoff in putting additional bits to loaded good subchannels and unloaded not-so-good subchannels, as the required energy to transmit one more bit increases as the modulation constellation size increases. Mathematically, the bit loading is done recursively as follows.

$$b_k = 0, \quad 1 \leq k \leq M$$

While $B > 0$,

$$\{$$

$$k^* = \arg\min_k \left[(P(b_k + \Delta b) - P(b_k)) / \Phi_k^2 \right];$$

$$b_{k^*} = b_{k^*} + \Delta b;$$

$$B = B - \Delta b;$$

$$\}$$

where $P(b_k)$ is the required energy to transmit b_k bits for a target BER with some type of modulation, and Δb is the bit allocation base unit.

2. After bit allocation, the total transmit power is allocated among the links in such a way that each link achieves the same minimum Euclidean distance in modulation and thus the same BER. Intuitively the system performance is limited by the worst subchannel. Therefore, the aggregate performance is approximately maximized with equal BERs in all used subchannels.

This link adaptation scheme can be readily extended to the scenarios when more detailed channel knowledge is available. For the SVD approach, we replace $\{\Phi_k\}$ by $\{\lambda_k\}$, the singular values of the channel matrix.

SVD signaling scheme requires feedback of instantaneous channel information, which may consume significant system bandwidth. Alternatively, computation can be done at the receiver side, and the information of the selected link adaptation modes is fed back only when they are different from the currently used ones. This approach trades the computational complexity at the receiver side for the system feedback overhead. But a MIMO receiver typically involves computations for decoupling and detection of the simultaneously transmitted data streams anyway (like V-BLAST), so link adaptation can be efficiently incorporated at the receiver side. We thus propose a link adaptation scheme based on zero-forcing (ZF) V-BLAST detection at the receiver. Assuming no error propagation, ZF V-BLAST successively decomposes the channel into a set of subchannels given by

$$y_k = \mathbf{w}_k^H * \mathbf{r}_k = x_k + \mathbf{w}_k^H * \mathbf{n}, \quad 1 \leq k \leq M, \quad (29)$$

where $\mathbf{r}_k$ is the detection vector for the k-th substream, a consequence of subtracting previously detected substreams from the received vector, and $\mathbf{w}_k^H$ is the nulling vector for the non-detected interfering substreams with $\mathbf{w}_k^H \mathbf{h}_k = 1$. Therefore, the link adaptation algorithm above can be readily applied, with $\{\Phi_k^2\}$ substituted by $\left\{ 1 / \|\mathbf{w}_k\|^2 \right\}$, which is proportional to the post-detection SNR of the subchannels in ZF V-BLAST detection.

To illustrate the effectiveness of our proposed link adaptation methods for D-MIMO, the BER performances of the above signaling schemes are compared for a $(1,4,4)$ C-MIMO and a $(4,1,4)$ D-MIMO as shown in Fig. 4, with spectral efficiency of 8 bits/s/Hz. For

simplicity we consider only square QAM modulation, indicating $\Delta b = 2$ in link adaptation algorithms. The detection technique is ZF V-BLAST except for the SVD signaling, where decoupled subchannels are seen.
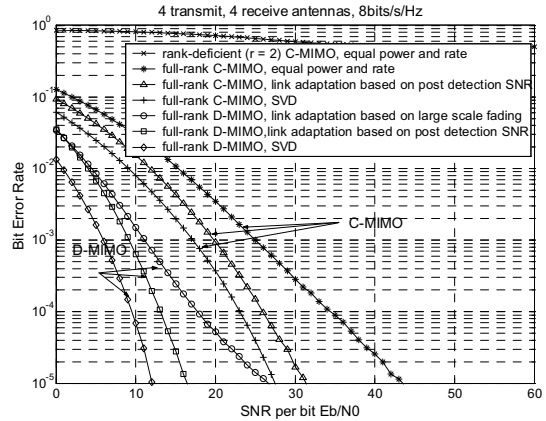

Fig. 4 Performance of link adaptation Schemes in C-MIMO and D-MIMO

As we see, for a rank-deficient C-MIMO channel (rank 2 in this case), the equal-power equal-rate signaling exhibits much inferior performance as not all independent substreams can be recovered after passing through the channel. For a full-rank C-MIMO channel, there is a significant performance gap between equal-power equal-rate signaling and optimal SVD signaling (about 15 dB at a BER of 10^{-5}), indicating the advantages of having CSI at the transmitter side to enable link adaptation techniques.

The most exciting result we obtain is that, link adaptation only based on macroscopic channel knowledge in D-MIMO (lower bound for link adaptation in D-MIMO) performs even better than link adaptation based on SVD in C-MIMO (upper bound for link adaptation in C-MIMO) in a large range of interest. This advantage results from the macrodiversity in D-MIMO, which is not available in a C-MIMO system. As we mentioned, this link adaptation scheme can be efficiently implemented, offering an excellent tradeoff between performance and complexity.

Finally we notice that more detailed channel knowledge at the transmitter side of D-MIMO can be traded for even higher performance gain. The gap between SVD-based and post-SNR based schemes may be partly due to the error propagation in V-BLAST detection.

V. CONCLUSION AND FUTURE WORK

This work provides some quantitative results to demonstrate the benefits of employing distributed MIMO systems in correlated fading and shadowing environments. Though the results rely on asymptotic analysis, they match simulation results quite well, as observed in literature and our work [13]-[18].

Extensions of current work include joint study of correlated fading and shadowing, the cooperative processing potential, and the outage capacity-scheduling gain tradeoff in D-MIMO.

APPENDIX A PROOF OF THEOREM 1

Proof: By Theorem 2 in [14], for C-MIMO with pure Rayleigh fading

$$\frac{\left[I_{eq}(\mathbf{H}) - \mu_1\right]}{\sigma_1} \xrightarrow{D} \mathcal{N}(0,1) . \tag{30}$$

So (18) follows readily from (17).

When shadow fading is considered for C-MIMO, it is observed that the instantaneous channel capacity conditioned on Φ is Gaussian distributed with mean $\mu(\Phi) = N \log \Phi + \mu_1$ and standard deviation σ_1. So the outage probability is given by

$$p = E\left\{ Q\left(\frac{N \log \Phi + \mu_1 - C_{C,S}^{(p)}}{\sigma_1} \right) \right\}, \tag{31}$$

where $\ln \Phi \sim \mathcal{N}(\lambda \mu_L, (\lambda \sigma_L)^2)$ for Log-normal shadow fading. (19) is obtained through

$$E\{Q(\eta + \gamma X)\} = Q\left(\frac{\eta}{\sqrt{1 + \gamma^2}} \right) \tag{32}$$

with $X \sim \mathcal{N}(0,1)$.

For D-MIMO, following a similar approach as in [14] (through applications of laws of large numbers and central limit theorem), it can be shown that

$$\frac{\left[I_{eq}(\mathbf{H}) - \mu'\right]}{\sigma'} \xrightarrow{D} \mathcal{N}(0,1), \tag{33}$$

where

$$\mu' = N \log(1 + \rho E\{\Phi\}), \tag{34}$$

and

$$\sigma' = \frac{\rho \log e \sqrt{(N + N^2)E\{\Phi^2\} - N^2 E^2\{\Phi\}}}{\sqrt{M}(1 + \rho E\{\Phi\})} . \tag{35}$$

At high SNR, through (6), we have

$$\mu' \approx \mu_1 + N\left(\lambda \mu_L + \frac{\lambda^2 \sigma_L^2}{2} \right) \log e , \tag{36}$$

and

$$\sigma' \approx \log e \sqrt{\frac{N}{M}[(1+N)e^{\lambda^2 \sigma_L^2} - N]} . \tag{37}$$

APPENDIX B PROOF OF THEOREM 2

Proof: By Theorem 3 in [14], for C-MIMO with pure Rayleigh fading

$$\frac{\left[I_{eq}(\mathbf{H}) - \mu_2\right]}{\sigma_2} \xrightarrow{D} \mathcal{N}(0,1) . \tag{38}$$

So (23) follows readily from (17). (24) is obtained through the same approach as Appendix A.

For D-MIMO, following similar steps in [13][14], it can be shown that

$$\frac{\left[I_{eq}(\mathbf{H}) - \mu''\right]}{\sigma''} \xrightarrow{D} \mathcal{N}(0,1), \tag{39}$$

and we are left to calculate the mean μ'' and standard deviation σ'' of $I_{eq}(\mathbf{H}) = \log \det\left(\mathbf{I} + \frac{\rho}{M} \mathbf{H}_w \mathbf{\Phi} \mathbf{H}_w^H \right)$.

If $\beta \leq 1$, we have

$$\sigma''^2 = \sigma_2^2 + M\left(E\{\log^2 \Phi\} - E^2\{\log \Phi\} \right)$$
$$= \sigma_2^2 + M\lambda^2 \sigma_L^2 \log^2 e . \tag{40}$$

If $\beta > 1$ we can only express σ'' as σ_D.

Determination of μ'' is facilitated through random matrix theory. Define the empirical distribution function of the eigenvalues of a square matrix $\mathbf{A}$ of size M as $F^{\mathbf{A}}(x) = \frac{1}{M} \#(\lambda_{\mathbf{A}} \leq x)$ (referring to the proportion of eigenvalues of $\mathbf{A}$ that lie below x). Then (c.f. (5))

$$F^{\mathbf{\Phi}}(x) \xrightarrow{a.s.} F_{\Phi}(x) \text{ as } M \to \infty . \tag{41}$$

By results of [15][16], as $M, N \to \infty$, with $M/N \to \beta$,

$$F^{(1/N)\mathbf{H}_w \mathbf{\Phi} \mathbf{H}_w^H}(x) \xrightarrow{a.s.} G(x), \tag{42}$$

where $G(x)$ is a deterministic distribution function such that its Stieltjes transform $m_G : \mathbb{C}^+ \to \mathbb{C}^{+\,2}$, defined as

$$m_G(z) = E_G\left\{ \frac{1}{X - z} \right\} = \int \frac{1}{x - z} dG(x), \tag{43}$$

satisfying

$$m_G(z) = \frac{1}{-z + \beta E\left(\dfrac{\Phi}{1 + \Phi m_G(z)} \right)}, \ z \in \mathbb{C}^+ . \tag{44}$$

Define

$$\eta(\rho) = \frac{\beta}{\rho} m_G\left(-\frac{\beta}{\rho} \right). \tag{45}$$

Following a similar approach as in [17], it can be shown that

$$I_{eq}(\mathbf{H}) \xrightarrow{a.s.} N\left[\beta E\left\{ \log\left(1 + \frac{\rho}{\beta} \eta \Phi \right) \right\} - \log \eta + (\eta - 1)\log e \right]. \tag{46}$$

Furthermore, at high SNR, we have

$$\eta(\rho) = \begin{cases} 1 - \beta & \beta < 1 \\ C_1 \rho^{-1/2} + O(\rho^{-1}) & \beta = 1 \\ C_2 \beta \rho^{-1} + o(\rho^{-1}) & \beta > 1, \end{cases} \tag{47}$$

where $C_1 = \sqrt{E\{1/\Phi\}}$, and C_2 is the same as given in (26). Plug (47) in (46) we can obtain the expression for the mean in (25) after some manipulation.

REFERENCES

[1] D. Gesbert, M. Shafi, D. Shiu, P. J. Smith, and A. Naguib, "From theory to practice: An overview of MIMO space-time coded wireless systems," *IEEE J. Select. Areas Commun.*, vol. 21, no. 3, pp. 281-302, Apr. 2003.

[2] A. Goldsmith, S. A. Jafar, N. Jindal, and S. Vishwanath, "Capacity Limits of MIMO Channels", *IEEE J. Select. Areas Commun.*, vol. 21, no. 5, pp. 684-702, June 2003.

[3] A. J. Paulraj, D. Gore, R. Nabar and H. Bolcskei, "An overview if MIMO communications – A key to Gigabit wireless," *Proc. IEEE*, vol. 92, no. 2, pp. 198-218, Feb. 2004.

---

[2] $\mathbb{C}^+$ is the set of complex numbers with non-negative imaginary parts.

[4] D. Shiu et al., "Fading correlation and its effect on the capacity of multi-element antenna systems," *IEEE Trans. Communications*, vol. 48, no. 3, pp. 502-513, March 2000.

[5] C.-N. Chuah, D. N. C. Tse, J. M. Kahn, and R. A. Valenzuela, "Capacity scaling in MIMO wireless systems under correlated fading," *IEEE Trans. Info. Theory*, vol. 48, no. 3, Mar. 2002.

[6] W. Roh and A. Paulraj, "Outage performance of the distributed antenna systems in a composite fading channel," *Proc. 2002 Fall IEEE Vehicular Technology Conference*, vol. 3, pp. 1520 -1524, Vancouver, Canada, Sept. 2002.

[7] H. Zhang and H. Dai, "On the Capacity of Distributed MIMO Systems," *Proc. 2004 Conference on Information Sciences and Systems* (CISS), Princeton University, Princeton, NJ, March 2004.

[8] A. Saleh, A. Rustako, and R. Roman, "Distributed Antennas for Indoor Radio Communication," *IEEE Trans. Communications*, vol. 35, no. 12, pp. 1245 -1251, Dec. 1987.

[9] M. V. Clark et al, "Distributed versus centralized antenna arrays in broadband wireless networks," *Proc. 2001 Spring IEEE Vehicular Technology Conference.*, pp. 33-37, Rhodes, Greece, May 2001.

[10] U. Grenander and G. Szegö, *Toeplitz Forms and Their Applications*, New York: Chelsea Publish, 1958.

[11] H. Bolcskei, D. Gesbert and A. J. Paulraj, "On the capacity of OFDM-based spatial multiplexing systems," *IEEE Trans. Commun.*, vol. 50, no. 2, pp. 225 -234, Feb. 2002.

[12] I. S. Gradshteyn and I. M. Ryzhik, *Table of Integrals, Series, and* Products, San Diego, CA: Academic, 2000.

[13] J. W. Silverstein and Z. D. Bai, "CLT of linear spectral statistics of large dimensional sample covariance matrices'", *Annals of Probability* **32**(1A) (2004), pp. 553-605.

[14] B. M. Hochwald, T. L. Marzetta and V. Tarokh, "Multi-Antenna channel hardening and its implications for rate feedback and scheduling", *IEEE Trans. Info. Theory*, vol. 50, pp. 1893-1909, Sept. 2004.

[15] J. W. Silverstein and Z. D. Bai, "On the empirical distribution of eigenvalues of a class of large dimensional random matrices," *J. Multivariate Anal.*, vol. 54, pp. 175-192, 1995.

[16] J. W. Silverstein and S. I. Choi, "Analysis of the limiting spectral distribution of large dimensional random matrices," *J. Multivariate Anal.*, vol. 54, pp. 295-309, 1995.

[17] S. Shamai (Shitz) and S. Verdú, "The impact of frequency-flat fading on the spectral efficiency of CDMA," *IEEE Trans. Inform. Theory*, vol. 47, no. 3, pp.1302-1327, May 2001.

[18] H. Dai, "On the duality between outage capacity and multiuser scheduling gain for MIMO systems and the impact of shadowing fading," *2005 Allerton Conference on Communication, Control and Computing*, Monticello, IL, Sept. 2005.

[19] H. Dai, "Distributed versus co-located MIMO systems with correlated fading and shadowing," *Proc. 2006 IEEE International Conference on Acoustics, Speech, and Signal Processing* (ICASSP), Toulouse, France, May 2006.

Huaiyu Dai received the B.E. and M.S. degrees in electrical engineering from Tsinghua University, Beijing, China, in 1996 and 1998, respectively, and the Ph.D. degree in electrical engineering from Princeton University, Princeton, NJ in 2002. He worked at Bell Labs, Lucent Technologies, Holmdel, NJ, during the summer of 2000, and at AT&T Labs-Research, Middletown, NJ, during the summer of 2001. Currently he is an Assistant Professor of Electrical and Computer Engineering at NC State University.

His research interests are in the general areas of communication systems and networks, advanced signal processing for digital communications, and communication theory and information theory. His current research focuses on distributed signal processing and crosslayer design (with a physical layer emphasis) in wireless ad hoc and sensor networks, distributed, multicell, multiuser MIMO communications, and associated information-theoretic and computation-theoretic analysis.

Hongyuan Zhang received the B.E. in electronic engineering from Tsinghua University, Beijing China in 1998, the M.S. in electrical engineering from Chinese Academy of Sciences, Beijing China in 2001, and the PhD degree in electrical engineering from North Carolina State University, Raleigh NC, in 2006. From May 2005 to Aug 2006, he worked in Mitsubishi Electrical Research Labs, Cambridge MA. He is currently a senior DSP design engineer in the signal processing group, Marvell Semiconductor Inc., Santa Clara CA.

Dr. Zhang's research interests include the performance analysis and signal processing in MIMO systems; MIMO-OFDM systems in WLAN and WiMax networks; multiuser cellular systems, and cognitive radios. He authored or co-authored one book chapter, several journal and conference publications, and nine pending US patents. He was one of the key contributors for the antenna selection features in the IEEE 802.11n draft spec.

Quan Zhou received the B.E. degree from Northern Jiaotong University, Beijing, China, in 1998, the M.S. degree from Tsinghua University, Beijing, China in 2001, and the Ph.D. degree from North Carolina State University, Raleigh, NC in 2006, all in Electrical Engineering. Currently he is a senior DSP design engineer in the signal processing group, Marvell Semiconductor Inc., Santa Clara CA.

His research interests are in the general areas of wireless MIMO communications with emphasis on link adaptation and multiuser scheduling. His current research focuses on the design, analysis and implementation of 802.11n system.